Proceeding of the IEEE
International Conference on Robotics and Biomimetics
Dali, China, December 2019

Swimming Characteristics of Soft robot with Magnetoelastic Material

Hongbiao Xiang[12*], Mengwei Li[12], Tilei Zhang[1], Shoujun Wang[12], Xiuping Yang[12]

1. Tianjin Key Laboratory for Advanced Mechatronic System Design and Intelligent Control, School of Mechanical Engineering
Tianjin University of Technology
Tianjin, 300384, China
xhb@tju.edu.cn

2.National Demonstration Center for Experimental Mechanical and Electrical Engineering Education
Tianjin University of Technology
Tianjin, 300384, China

***Abstract* - Cable-less micro-robots have exhibit great capabilities for remote applications in small and constrained environments, especially in biotechnology and healthcare. This paper presents a swimmer propelled by its undulatory deformation using magnetoelastic composite material. The robot can move freely on water surface driven through a function of magnetic field, such as forward, backward and steering with different velocity. The magnetic field is generated by 3D Helmholtz coils, and the locomotion of the micro swimming robot is controlled by different applied magnetic field. To understand the characteristics of the swimmer, the force balance equation is established, and the morphologies of swimmer with different magnetic field are analyzed and described through finite element analysis method. Furthermore, we discuss and analyze relationship between the parameters of magnetic field and the speed of the swimmer. The experimental results verified the speed model of the swimming robot, which is influenced by the frequency and strength of magnetic field.**

Index Terms* - *Soft robot, Swimmer, Magnetic control, Magnetoelastic composite material

I. INTRODUCTION

Unlike conventional actuators and robots, micro-robots can work in a small and complex space in various biomedical areas and micro-factories [1]. However, rigid materials are hard to achieve multi-locomotion for micro-robots. Smart flexible materials are promising candidates to address these challenges since they can be untethered driven by for multiple functionalities. Therefore, micro-soft robots [2], as a new frontier subject involving materials, machinery, biological medicine and other fields, have attracted extensive attention by many researchers in recent years [3-5].

Due to the small size of the micro-swimming robot, it is difficult to realize the on-board energy supply and drive on the micro-robot, how to solve energy supply and drive problem is one of the most important tasks in the micro-robot field. At present, researchers have proposed some tetherless control methods to drive the micro-robot by using microorganism [6], chemical reaction [7] and magnetic field [8-11]. The micro underwater robot produced by Guo in Japan using Ionic Conducting Polymer Film (ICPF) materials can move in water when the applied voltage control signal is applied [12]. Hwang uses the electroosmotic force generated by the electric field to push the micro-robot to swim with a swimming speed of up to 1.8mm/s [13]. Diller et al. developed a millimeter magnetic driving swimming robot and provided an effective remote actuating method to control the robot [14]. Xu et al. proposed a spiral micro cone based on lotus root, which was formed by the activation of magnetic nanoparticles coated on the fiber surface of lotus root under the control of magnetic field, and found that the curvature of the robot shape decreased with the change of excitation field frequency [15]. Zhang et al. made a micro-soft robot using flexible magnetic homogeneous composite materials, and proved the swimming ability and operability of the robot through experiments, and quantitatively characterized its swimming performance under various conditions [16]. Ye et al. demonstrated that a potential way to improve the swimming performance of the spiral micro-swimming robot is to increase its hydrophobic surface [17]. Among the many strategies that have been proposed for these problem, magnetic fields have become a preferable option. In this paper, a kind of micro swimming robot based on magnetoelastic composite material is proposed and manufactured. The control strategies of the micro-swimming robot are carried out through the 3D Helmholtz coils. We focus on characteristics and morphology of swimmer through finite element analysis and modelling compared with the experiments.

In the following article, Section II introduces the structure of the micro-swimming robot and establishes the mathematical model of the robot. Section III presents the experimental system and the control method. In the Section IV, the mechanical characteristics of the robot are explored, and the experimental results show the same trend with the effects of magnetic field strength and frequency of the model of robot's swimming speed. Finally, Section V is the conclusion.

II. STRUCTURE AND MODELING

A. Structure

The micro-soft swimming robot is composed of magnetic and flexible material. As shown in Fig.1, the magnetoelastic

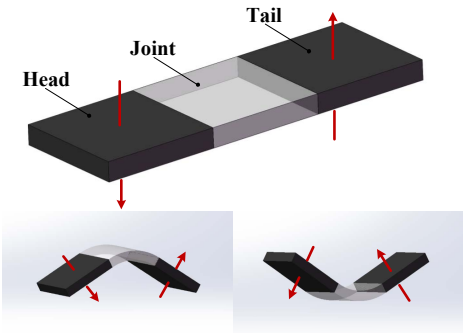

Fig. 1 Structure of soft robot

978-1-7281-6321-5/19//$31.00 ©2019 IEEE

composite material (YMM-E-15-7, NdFeB and Ecoflex 00-10) is cut into two magnetic blocks with the same size and opposite magnetization direction, and they are regarded as the head and tail of the robot. The joint part of the robot, which is linked the head and tail using silicone rubbers (Ecoflex 00-10).

The swimmer designed in this paper has the following characteristics. The magnetization direction of the head and tail of the robot is opposite and perpendicular to the horizontal plane. The robot is lying on the water in the absence of a magnetic field. Otherwise, when the uniform magnetic field is applied, the robot body can bend upward or downward on the water surface, combined with the action of external force and internal force. Therefore, the swimmer can move on the water surface with periodic external magnetic field, and it can realize forward, backward, steering locomotion and so on.

B. Force analysis

The performance of a soft robot is determined by its material properties, geometry structure and external magnetic field. Considering the head and tail parts of soft robots are rigid, hard to deform, the deformation of the swimmer mainly occurs in the joint part, because the joint is more flexible. The length of swimmer is 3L (L=3mm) and the height is D (D=0.5mm). The force analysis is shown in Fig. 2.

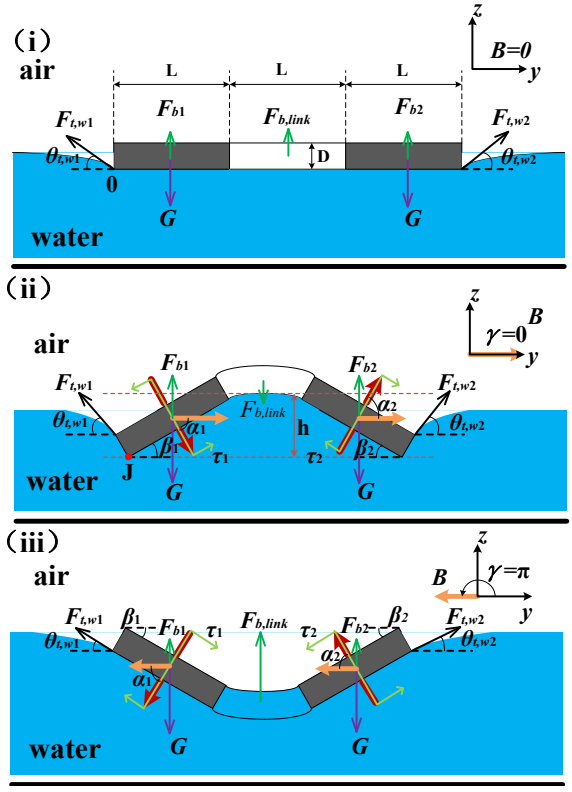

Fig. 2 Force analysis of the swimmer on water surface

The magnetic block is only subjected to the magnetic torque in a uniform magnetic field. Because of the opposite direction of magnetization of the magnetic block, the magnetic moment on the head and tail of the robot are different. They can be expressed by the following equation

$$\begin{cases} \tau_1 = MBV\sin\alpha_1 \\ \tau_2 = MBV\sin\alpha_2 \end{cases} \tag{1}$$

where M, B and V are the magnetization, magnetic flux density and the volume of the block respectively. α_1 and α_2 represent the angle between the magnetization direction of the head and tail magnetic block and the direction magnetic flux density B respectively.

The α_1 and α_2 can get as follows

$$\begin{cases} \alpha_1 + \beta_1 = \dfrac{\pi}{2} + \gamma \\ \alpha_2 + \beta_2 = \dfrac{\pi}{2} - \gamma \end{cases} \tag{2}$$

where β_1 represents the angle between the head and the horizontal plane, β_2 represents the angle between the tail and the horizontal plane respectively, and γ is the direction of the external magnetic field.

As is shown in Fig. 2, the swimmer is subjected the gravity, magnetic moment, buoyancy and surface tension of the water. To simplify the force analysis, we ignore the mass of joint because of its smaller density. The surface tension F_t exists at the boundary of the contact area between the swimmer and water. The direction of tension is the disturbance direction of the robot to the water surface, and the direction is tangent to the water surface at the contact point of the robot. The angle between tension and horizontal plane is θ_t. The tension on the width edge of the soft robot is expressed by $F_{t,w}$, and the angle between them and the horizontal plane is $\theta_{t,w}$. Since the force balance equation is based on the section of yz plane, in order to simplify the model, we only consider the effect of tension in the width direction of the swimmer. The resultant force of tension in the vertical direction is expressed by $F_{t,res}$. Buoyancy of the robot is represented by F_b. The buoyancy on the head and tail of the robot is F_{b1} and F_{b2} respectively. The buoyancy of the joint is $F_{b,link}$.

Considering the buoyancy is always perpendicular to the horizontal direction, we use $F_{b,res}$ to represent the resultant force of buoyancy. Based on quasi-static equilibrium equation, the force equation in yz plane is established.

$$\begin{cases} F_{t,res} + F_{b,res} = 2G \\ F_{t,res} = F_{t,w1}\sin\theta_{t,w1} + F_{t,w2}\sin\theta_{t,w2} \\ F_{b,res} = F_{b1} + F_{b2} + F_{b,link} \end{cases} \tag{3}$$

As is shown in Fig. 2(ii), the torque balance equation is established on point J as the reference point.

$$M_G + M_t + M_b + \tau_1 - \tau_2 = 0 \tag{4}$$

M_G is the torque of gravity on point J.

$$M_G = -\frac{3}{2}LG\cos\beta_1 - \left(w_{yL} + \frac{1}{2}L\cos\beta_2\right)G \tag{5}$$

M_t is the torque of tension on point J.

$$M_t = \left(L\cos\beta_1 + w_{yL} + \frac{1}{2}L\cos\beta_2 \right) F_{t,w2}\sin\theta_{t,w2} \quad (6)$$

M_b is the torque of buoyancy on point J.

$$M_b = \frac{L}{2}F_{b1}\cos\beta_1 + F_{b,link}\left(L\cos\beta_1 + \frac{w_{yL}}{2} \right) + F_{b2}\left(L\cos\beta_1 + w_{yL} + \frac{1}{2}L\cos\beta_2 \right) \quad (7)$$

where w_{yL} represents the distance of the joint in the y-axis direction. The joint will bend due to the combined force of the robot. According to the bending theory of beam, the distance along the axis of the beam is s ($s \in [0, L]$). α represents the angle of any point and vertical direction on the curved beam.

$$w_{yL} = \int_0^L \cos\alpha ds \quad (8)$$

According to Euler Bernoulli beam theory, the bending moment Q on the joint as

$$Q = \frac{d\alpha}{ds}\cdot EI \quad (9)$$

where EI is bending stiffness.

According to the swimming speed of Taylor model [18], the swimming speed model as follow

$$v = \frac{2\pi^2}{3L}(AR)^2 f = \frac{2\pi^2}{3L}\left(\frac{hR}{2}\right)^2 f \quad (10)$$

As is shown in Fig. 2(ii), the speed is affected by the magnetic field frequency and the amplitude of the undulation. We note that the bending degree as h, influenced by the strength of magnetic field, surface tension buoyancy and gravity. Then approximatively note that the bending degree is twice of the amplitude A of the Taylor model, which is use to describe the undulatory bending. The variables R represents the asymptotic approximation of the Bode magnitude function of ideal 2nd order systems. When the frequency of magnetic field is less than $\omega/2\pi$, the value of R is equal to 1. When the frequency of magnetic field is greater than or equal to $\omega/2\pi$, the value of R is $(\omega/2\pi f)^2$. The ω represents the lowest non-zero fundamental natural frequency of the swimmer (204.1 rad/s).

III. Control System Setup

A. Experiment system

The control part of the experimental system is shown in Fig. 3. The system is composed of Industrial Personal Computer(IPC), LabVIEW CompactDAQ (Laboratory Virtual Instrumentation Engineering Workbench， NI cDAQ-9174), power amplifier(HEA-1050), high speed camera(Mako U-130B) and 3D Helmholtz coils(3HLY5-130). The LabVIEW module outputs three voltage signals, which are transformed by the power amplifier into three pairs of orthogonal Helmholtz coils current control signals, so as to generate a uniform magnetic field in any direction in space, and construct the magnetic field environment required by various movement postures of the soft robot on the water surface.

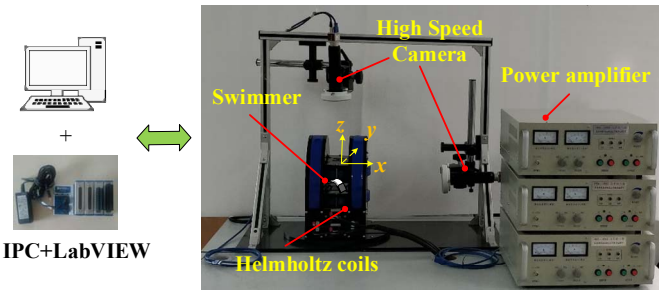

Fig. 3 Control system setup

B. Control strategy

Three pairs of orthogonal Helmholtz coils generate a uniform magnetic field in directions of XYZ. Spatial magnetic field sphere coordinate system (B, γ, φ) is established with XYZ three-channel control signals. B is the magnetic flux density of the external magnetic field. The angle of space uniform magnetic induction B with xy plane is γ, and the angle with xz plane is φ. Note that the counterclockwise direction is positive. The XYZ three-channel control signals are programmed in LabVIEW, and the angle and magnetic field can be arbitrarily changed to realize the output of arbitrary waveform. Therefore, we have written a program to control the straight motion and rotation of the swimmer on the water surface.

When the swimmer swims in a certain direction in the xy plane, the rotation magnetic field is parallel to the z-axis. The strength of magnetic field is constant, and the direction is rotating along γ counter-clockwise. In this way, the robot can swim arbitrarily on the water surface in xy plane. Changing the angle of φ space magnetic field in the xy plane can realize the steering motion of the swimmer on the water surface. In the other word, we can realize it by changing the rotation angle of the spatial magnetic field around the z axis, its principle is shown in Fig. 4.

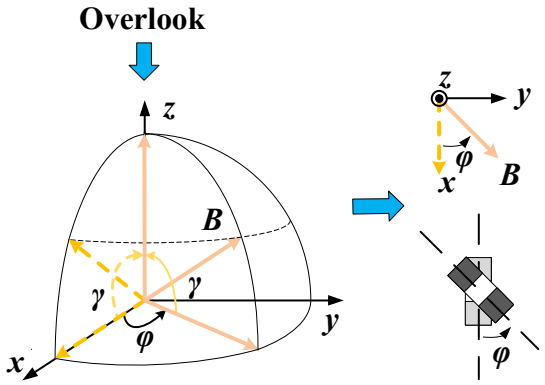

Fig. 4 Motion control at sphere coordinate system

IV. Experiment and Analysis

A. Analysis of Motion Characteristics

In order to explore the influence of magnetic field on the motion characteristics of soft robot, we use finite element method (FEM) by Abaqus in this paper. The mechanical properties of the concave and convex of the robot are analyzed on the water surface. When the magnetic field is parallel to the y-axis ($\gamma = 0$), the head and tail of the robot are in a symmetric state with the same value of magnetic moment. With the increasing of strength of magnetic field, the bending degree of the robot on the water surface also increases gradually. The comparison between experiment and FEM are shown in Fig. 5.

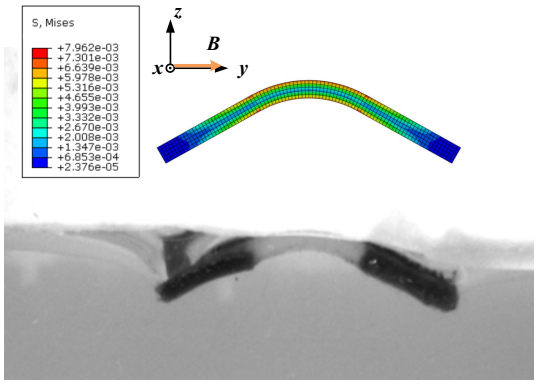

Fig. 5 Effect of magnetic field on robot attitude

The relationship between the bending degree of the soft robot and magnetic flux density are explored. The experimental results show that the experimental data is basically consistent with the simulation results. The bending degree increases with the magnetic flux density. According to the experimental results, a mathematical model between the bending degree and the magnetic flux density is established in this paper as shown in Fig. 6.

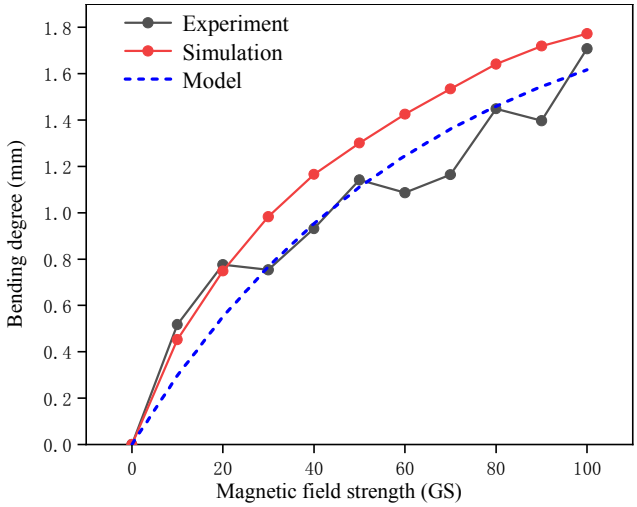

Fig. 6 The relationship between magnetic flux density and bending degree

The model as follows

$$h=\left(\frac{3L}{2}-D\right)\left(1-\frac{e^{-0.00011B}}{2}-\frac{e^{-0.01596B}}{2}\right) \tag{11}$$

According to the equation (10), we can update the swimming speed model

$$v=\frac{\pi^2}{6L}\left(\frac{3L}{2}-D\right)^2\left(1-\frac{e^{-0.00011B}}{2}-\frac{e^{-0.01596B}}{2}\right)^2 R^2 f \tag{12}$$

B. Analysis of swimming speed

A periodic time-varying rotation magnetic field is applied to the swimming robot on the water surface. By changing the parameters, including frequency, B, γ, and φ in the spherical coordinate system of the magnetic field, the motion direction and the swimming speed of the soft robot can be controlled.

Fig. 8 is shown 6 different states in one swimming motion cycle, compared the results between the experiments and FEM. The frequency and strength of magnetic field are 11Hz and the 70Gs respectively. Note that the positive rotate direction is counterclockwise. The position and posture of the robot are obtained when the direction of magnetic field is 0 degree, 60 degree, 120 degree, 180 degree, 240 degree and 300 degree, respectively. The concave convex properties are shown with the periodic undulatory bending on the surface of the water. As shown as Fig. 7, compared with the experiment and FEM results, we can get almost the same morphologies in one swimming cycle. Therefore, according the method above, the robot can swim arbitrarily on the water surface with the different input signals.

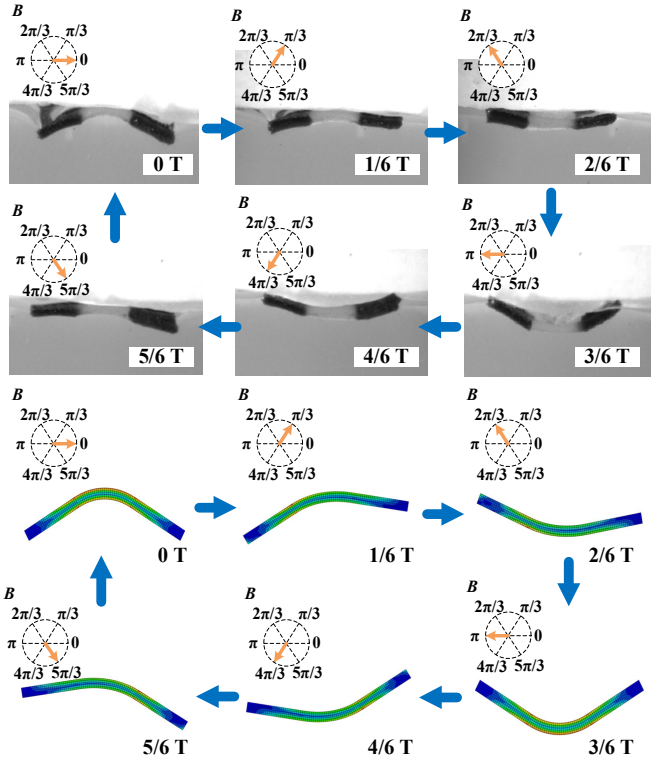

Fig. 7 Swimming process of experiment and FEM

When the magnetic field frequency is constant, the relationship between swimming speed and magnetic field strength are obtained. As shown in Fig. 8, When the frequency of driving magnetic field is 11Hz, the swimming speed of the robot on the water surface increases gradually with the increase of the strength of magnetic field. we can get the functional relationship between the strength of magnetic field and the swimming speed, and experimental results approximatively follows the trend with the speed model (12).

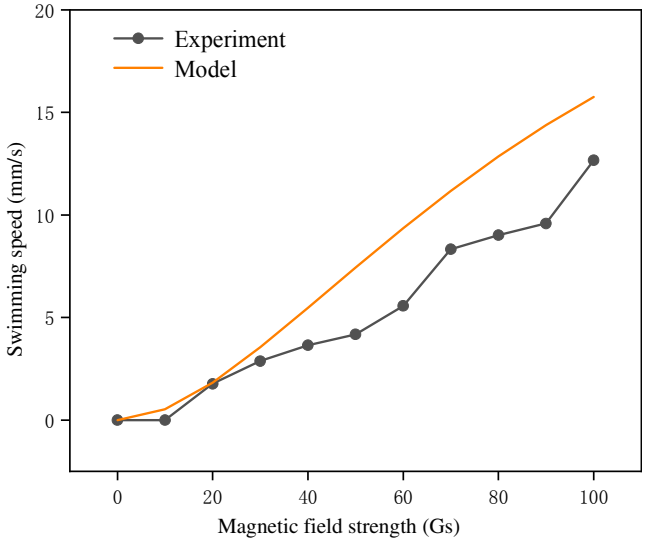

Fig. 8 The relationship between magnetic field strength and swimming speed

When the magnetic field strength is constant, the relationship between swimming speed and magnetic field frequency can be obtained. Thus, the magnetic field strength is set to 70Gs, the influence of magnetic field frequency on the swimming speed of the robot is shown in Fig. 9. In the other word, when the magnetic field strength remains constant, the swimming speed is related to the *R*, that is, the natural frequency of the robot. Therefore, the motion speed of the robot on the water surface firstly increases with the increase of the magnetic field frequency, and then decreases with the increase of the magnetic field frequency.

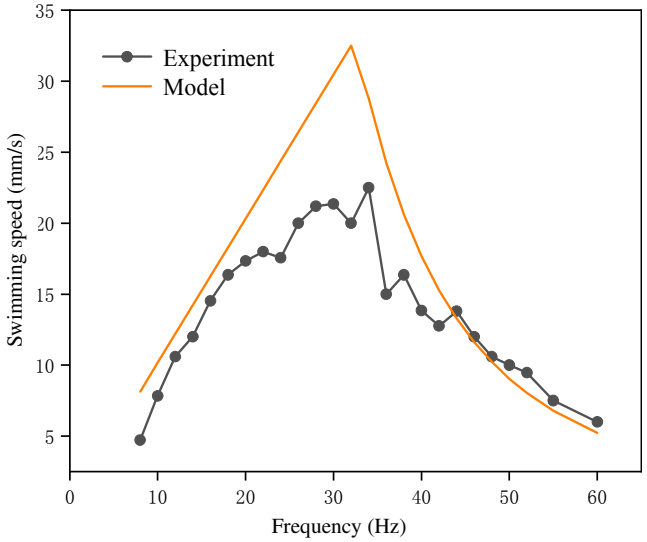

Fig. 9 The relationship between frequency and swimming speed

C. *Steering motion*

Fig. 10 is an example of steering motion control strategy, and the robot can swim along the trajectory of *xy* plane with the three input signals of XYZ axis. The angle φ are chosen at 0 degree, 60 degree, 120 degree, 180 degree, 240 degree and 300 degree, and each of the waveforms last for one second. The composite waveform of XY channel is cosine waveform, and the Z channel is sine waveform.

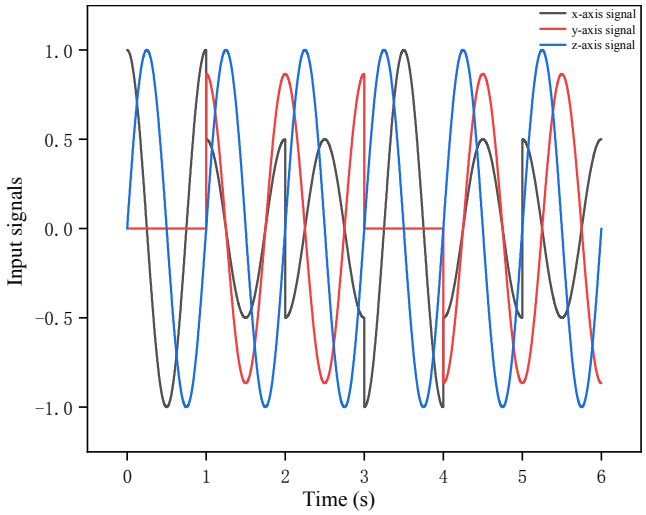

Fig. 10 Input signals of 3D Helmholtz coils

Following the output signal of Fig. 10, we recorded the trajectory of the swimmer. According to the XYZ control signals of Fig. 10, the ideal path is a regular hexagon track (red line) based on the model (12), and the following path experiment of swimmer is green line. As shown in Fig. 11, the experimental results are approximatively consistent with the model path, and the larger deviation appears in the angle changing corner.

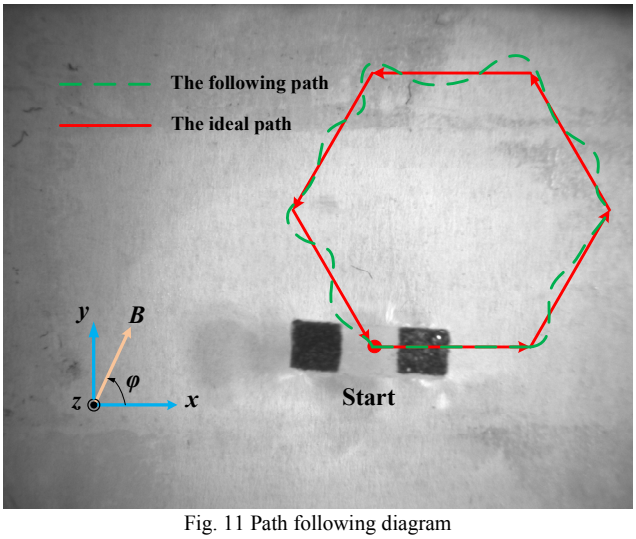

Fig. 11 Path following diagram

V. CONCLUSION

This paper analyzes the law of motion and the change of the magnetic field of the micro-soft swimming robot, establish the mathematical model of the robot, and design the control strategy of magnetic field. The mechanical model of the swimmer is established and verified by FEM and experiments. Firstly, the mechanical analysis of the robot is carried out, and the relationship between the bending degree of the swimmer and the magnetic field strength is obtained. Then we analyze the relationship between the frequency, strength of magnetic field, and the swimming speed respectively. Finally, the experimental results are basically consistent with the theoretical model. However, there is still a certain deviation between the model and experiments, mainly because the manufacturing precision of the micro-robot is not perfect enough. Furthermore, the future work will focus on the closed-loop control to improve the control precision of the swimmer. The above conclusions and research results are of guiding significance and reference value to further promote the research of the soft robot with magnetic material.

ACKNOWLEDGMENT

The author would like to thank Tianjin University of technology and Tianjin University, and this work was supported by National key research and development Program of China under Grant (NO.2017YFB1302100) and Tianjin Natural Science Foundation (NO.18JCYBJC19300).

REFERENCES

[1] S. Tottori, et al, "Magnetic Helical Micromachines: Fabrication, Controlled Swimming, and Cargo Transport," *Advanced Materials*, vol. 24, no. 6, pp. 811-816, 2012.

[2] J. M. Breguet, W. Driesen, F. Kaegi, T. Cimprich, "Applications of Piezo-Actuated Micro-Robots in Micro-Biology and Material Science," in *2007 IEEE International Conference on Mechatronics and Automation (ICMA)*, pp. 57-62, 2007.

[3] H. Xiang, M. Trkov, K. Yu, and J. Yi, "A stick-slip interactions model of soft-solid frictional contacts," *Journal of Dynamic Systems, Measurement, and Control,* vol. 141, no. 4, 2019.

[4] H. Xiang, J. Ba, Y. Li, T. Zhang, S. Wang, "Study on Tetherless Micro-Soft Robot Based on Magnetic Elastic Composite Material," in *2019 IEEE International Conference on Mechatronics and Automation (ICMA)*, pp. 673-688, 2019.

[5] D. Hilbich, A. Rahbar, A. Khosla, B. L. Gray, "Manipulation of permanent magnetic polymer micro-robots: A new approach towards guided wireless capsule endoscopy," *Progress in Biomedical Optics and Imaging - Proceedings of SPIE*, vol. 8548, 2012.

[6] B. J. Williams, S. V. Anand, J. Rajagopalan, M. T. A. Saif, "A self-propelled biohybrid swimmer at low Reynolds number," *Nature Communications*, 2014, 5:4081.

[7] A. A. Solovev, et al, "Self-Propelled Nanotools," *ACS Nano*, vol. 6, no. 2, pp. 1751-1756, 2012.

[8] V. M. Fomin, E. J. Smith, D. Makarow, S. Sanchez, O. G. Schmidt, "Dynamics of radial-magnetized microhelix coils," *Physical review B, Condensed matter*, vol 84, no. 17, pp. 4388-4396, 2011.

[9] K. E. Peyer, "Bacteria-Inspired Magnetic Polymer Composite Microrobots," in *Proceedings of the Second international conference on Biomimetic and Biohybrid Systems*, vol. 8064, pp. 216-227, 2013.

[10] M. Suter, et al, "Superparamagnetic microrobots: fabrication by two-photon polymerization and biocompatibility," *Biomedical Microdevices*, vol.15, no. 6, pp.997-1003, 2013.

[11] C. Peters, O. Ergeneman, B. J. Nelson, C. Hierold, "Superparamagnetic swimming microrobots with adjusted magnetic anisotropy," in *2013 IEEE International Conference on Micro Electro Mechanical Systems (MEMS)*, pp. 564-567, 2013.

[12] S. Guo, et al, "Micro Active Guide Wire Catheter System -Characteristic Evaluation, Electrical Model and Operability Evaluation of Micro Active Catheter", in *1996 IEEE International Conference on Robotics and Automation (ICRA)*, vol. 3, pp. 2226-2231, 1996.

[13] G. Hwang, et al, "Electro-Osmotic Propulsion of Helical Nanobelt Swimmers," *International Journal of Robotics Research*, vol. 30, no. 7, pp. 806-819, 2011.

[14] E. Diller, J. Zhuang, G. Zhan Lum, M. R. Edwards, "Continuously distributed magnetization profile for millimeter-scale elastomeric undulatory swimming," *Applied Physics Letters*, vol. 104, no. 17, 2014.

[15] J. Liu, T. Xu, Y. Guan, X. Yan, C. Ye, and X. Wu, "Swimming Characteristics of Bioinspired Helical Microswimmers Based on Soft Lotus-Root Fibers," *Micromachines*, vol. 8, no. 12, 2017.

[16] J. Zhang, and E. Diller, "Untethered Miniature Soft Robots: Modeling and Design of a Millimeter-Scale Swimming Magnetic Sheet," *Soft Robotics*, vol. 5, no. 6, pp. 761-776, 2018.

[17] C. Ye, et al, "Hydrophobicity Influence on Swimming Performance of Magnetically Driven Miniature Helical Swimmers," *Micromachines*, vol. 10, no. 3, 2019.

[18] G. Taylor, "Analysis of the Swimming of Microscopic Organisms," *Proceedings of the Royal Society A: Mathematical, Physical and Engineering Sciences*, vol. 209, no. 1099, pp. 447-461, 1951.